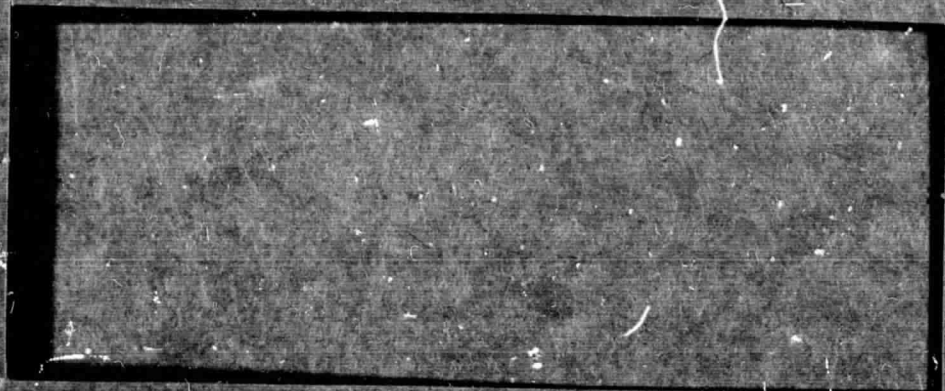


General Disclaimer

One or more of the Following Statements may affect this Document

- This document has been reproduced from the best copy furnished by the organizational source. It is being released in the interest of making available as much information as possible.
- This document may contain data, which exceeds the sheet parameters. It was furnished in this condition by the organizational source and is the best copy available.
- This document may contain tone-on-tone or color graphs, charts and/or pictures, which have been reproduced in black and white.
- This document is paginated as submitted by the original source.
- Portions of this document are not fully legible due to the historical nature of some of the material. However, it is the best reproduction available from the original submission.



FACILITY FORM 602

N71-34982

(ACCESSION NUMBER)

40

CR-119896

(PAGES)

(NACA C, CR, TMX OR AD NUMBER)

G3

(F.R.U.)

(CODE)

32

(CATEGORY)

MCDONNELL DOUGLAS



CORPORATION

CR-119896

Copy number 22

Report number MDC A0938

A Method for Predicting the Panel Flutter Fatigue Life
of
Saturn V Panels

Revision date

Revision letter

Issue date 22 February 1971

Contract number

Prepared by

Hans P. Kappus C. E. Lemley N. H. Zimmerman
H. P. Kappus, C. E. Lemley, N. H. Zimmerman

Approved by

C. H. Perisho
C. H. Perisho

Prepared by
MCDONNELL DOUGLAS CORPORATION
McDonnell Aircraft Company
St. Louis, Mo.
Under Contract No. NAS8-21250
for
George C. Marshall Space Flight Center
Marshall Space Flight Center, Alabama, 35812

MCDONNELL AIRCRAFT COMPANY

Box 516, Saint Louis, Missouri 63166 - Tel. (314)232-0232

MCDONNELL DOUGLAS

CORPORATION



SUMMARY

This report, prepared under NASA Contract NAS8-21250, describes a procedure for estimating the fatigue life of fluttering panels by using both theoretical and experimental data. The procedure includes techniques for estimating panel flutter onset dynamic pressure and for estimating surface stresses of panels deep in flutter. Application of this procedure should yield conservative results because of the following assumptions made in its formulation: panels are loaded to buckling; no static pressure differential exists across panel; boundary layer has negligible effect; local aerodynamic conditions are assumed equal to freestream.

The procedure was applied to skin panels typical of those on the Saturn V launch vehicle using the Apollo lunar trajectory. Even though panels of several different geometries were found to penetrate into the flutter region, no fatigue failures were predicted. The predicted level of fatigue damage due to flutter was low enough for all the geometries examined to ensure at least five missions before a skin panel failure.

DEFINITION OF SYMBOLS

| <u>Symbol</u> | <u>Definition</u> | <u>Units</u> |
|---------------|---|--------------------------|
| D | $= \frac{Et^3}{12(1-\mu^2)}$, flexural rigidity of panel | Pound-Inch |
| E | Modulus of elasticity | Pounds/Inch ² |
| F | $= \frac{q_o}{E} \left\{ \frac{L}{t} \right\}^3$, non-dimensional flutter function | ----- |
| H | = $\Sigma \Delta H$, Miner's fatigue damage index | ----- |
| K | = q_{on}/q_o , buckling correction factor | ----- |
| L | Panel stream direction dimension | Inches |
| M | Freestream Mach number | ----- |
| N | Number of stress cycles required for fatigue failure | ----- |
| n | Number of stress cycles at a given stress condition | ----- |
| \bar{P} | $= \frac{\Delta PW^4}{Dt}$, static pressure parameter | ----- |
| q | Freestream dynamic pressure | Pounds/Inch ² |
| q_o | Flutter onset dynamic pressure for unloaded Panel | Pounds/Inch ² |
| q_{on} | Flutter onset dynamic pressure for buckled panel | Pounds/Inch ² |
| \bar{q} | $= \frac{(q - q_{on}) W^4}{Dt}$, flutter penetration factor | ----- |
| t | Panel thickness | Inches |
| W | Panel cross-stream dimension | Inches |
| ω_f | Flutter frequency | Radians/Second |

| <u>Symbol</u> | <u>Definition</u> | <u>Units</u> |
|---------------------|--|---|
| β | $= \sqrt{M^2 - 1}$, supersonic compressibility factor | ----- |
| ΔH | $= \frac{(\omega_f/\pi) \Delta t}{N}$, fatigue damage at a given stress condition | ----- |
| ΔP | Differential pressure across panel | Pounds/Inch ² |
| Δt | Time interval | Seconds |
| Λ | Freestream dynamic pressure over flutter onset dynamic pressure | ----- |
| μ | Poisson's ratio | ----- |
| Ω | $= \frac{\omega_f^2 \rho t L^3 W}{D}$, flutter frequency parameter | ----- |
| ρ | Panel mass density | $\frac{\text{Pound-Second}^2}{\text{Inch}^4}$ |
| $\sigma_{a_{\max}}$ | Maximum peak-to-peak surface stress | Pounds/Inch ² |
| σ_B | Maximum panel bending stress | Pounds/Inch ² |
| σ_M | Maximum panel membrane stress | Pounds/Inch ² |
| σ_{\max} | Maximum panel surface stress | Pounds/Inch ² |
| $\bar{\sigma}$ | $= \frac{\sigma_{\max} (1-\mu^2)}{E (t/W)^2}$, non-dimensional maximum surface stress | ----- |

TABLE OF CONTENTS

| | <u>Page</u> |
|---|-------------|
| 1. INTRODUCTION | 1 |
| 2. OVERVIEW OF CRITERION | 2 |
| 2.1 Background | |
| 2.2 Detailed Procedure | |
| 3. DEVELOPMENT OF PREDICTION METHOD | 7 |
| 3.1 Determination of the Flutter Onset Dynamic Pressure | |
| 3.2 Prediction of Stresses During Flutter | |
| 3.3 Estimation of Flutter Frequency | |
| 3.4 S-N Diagram | |
| 3.5 Conservatism | |
| 4. APPLICATION OF PROCEDURE TO SATURN V PANELS | 13 |
| 4.1 Criterion Input Information | |
| 4.1.1 Launch Trajectory | |
| 4.1.2 Panel Material Properties | |
| 4.1.3 Panel Geometries | |
| 4.1.4 Stress Concentration Factor | |
| 4.2 Results | |
| 4.2.1 Flutter Penetration | |
| 4.2.2 Maximum Alternating Stress | |
| 4.2.3 Flutter Frequency | |
| 4.2.4 Panel Fatigue Life | |
| 4.2.5 Effect of Changing Panel Width | |
| 4.3 Conclusion | |
| REFERENCES | 34 |

List of Pages

Title page

i - iv

1 - 34

1. INTRODUCTION

The design of skin panels that are subject to flutter has traditionally been governed by flutter onset criteria (see Reference 1 for example) which require that panel flutter be avoided. It was suspected about five years ago that some panels on the Saturn launch vehicle, and particularly on the S-IVB stage, might be flutter critical. However, no rational approach existed to assess whether or not panel failure might result. Recently, however, efforts have been made both theoretically (Reference 2) and experimentally (Reference 3) to determine the behavior of panels that are deep in flutter thereby offering the possibilities of predicting panel stresses and of predicting panel fatigue life.

This report describes a procedure that has been developed by the McDonnell Douglas Corporation (MDC) to assess the fatigue life of panels characteristic of the S-V vehicle and trajectory and presents the results of its application. The overall procedure involves (1) the estimation of panel flutter onset boundaries, (2) the estimation of stress time histories of fluttering panels as a function of Mach number and dynamic pressure, and (3) the use of Miner's cumulative fatigue concept to estimate fatigue life. The estimates of panel stress during flutter are derived mainly from wind tunnel tests reported in Reference (3) with theoretical extrapolation to panels of different thickness and length-to-width ratio. Detailed explanation of procedures is given later in this report.

The final results from the application of the fatigue criterion cover panels with the following ranges of physical characteristics:

Thickness: 0.02 to 0.055 inch

Length: 6.7 to 33.5 inches

Length-to-width ratio: 1 to 5

Material: 7075-T6 Aluminum

2. OVERVIEW OF CRITERION

This section presents a general approach that is used to assess the panel flutter integrity of Saturn V panels for both current and future missions. For extrapolation to future applications it is assumed that:

- a. Structural configurations of skin panels will be similar to the present configuration (i.e. edge restraints simulate the clamped condition, and panel curvature effect is negligible)
- b. Flow sweep angle with respect to panels remains small
- c. Cavity volume behind panels is large
- d. Each panel has uniform thickness and rectangular (or nearly rectangular) planform
- e. Boundary layer influence is negligible
- f. Panels do not have damping treatment
- g. No differential pressure across panel
- h. Panel compressive load is at or very near buckling
- i. Freestream q and M are used for local values

The last three assumptions add conservatism and were employed to simplify the application of the criterion.

2.1 Background

In a broad sense, the development of the fatigue criterion involved the following requirements:

- a. Define the aerodynamic environments and the structural characteristics for each panel or each class of panels
- b. Determine which panels will flutter and eliminate non-fluttering panels from further consideration
- c. For panels that will flutter, determine the time history of flutter penetration for the trajectory to be flown
- d. Determine maximum oscillatory bending and membrane stresses corresponding to flutter penetrations in (b) above. Determine corresponding frequencies; transform to cycles of oscillating stress
- e. From the cumulative stress-cycle calculations apply Miner's fatigue criteria to assess panel fatigue damage

Details of the step-by-step procedure are covered in the following paragraphs.

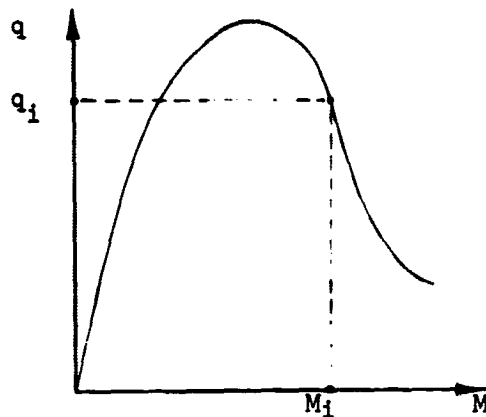
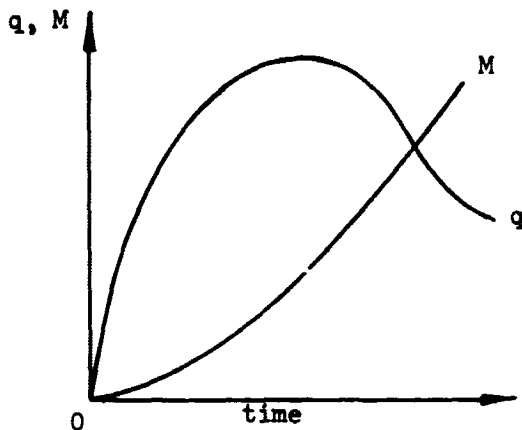
22 February 1971

2.2 Detailed Procedure

Step 1. Define Structural Input Information - The following structural input information is required:

- a. Panel material properties
 - Modulus of elasticity - E
 - Poisson's ratio - μ
 - Mass density - ρ
 - Fatigue curves
- b. Panel geometry
 - Thickness - t
 - Width (cross stream) - W
 - Length (streamwise) - L
- c. Stress concentration factor

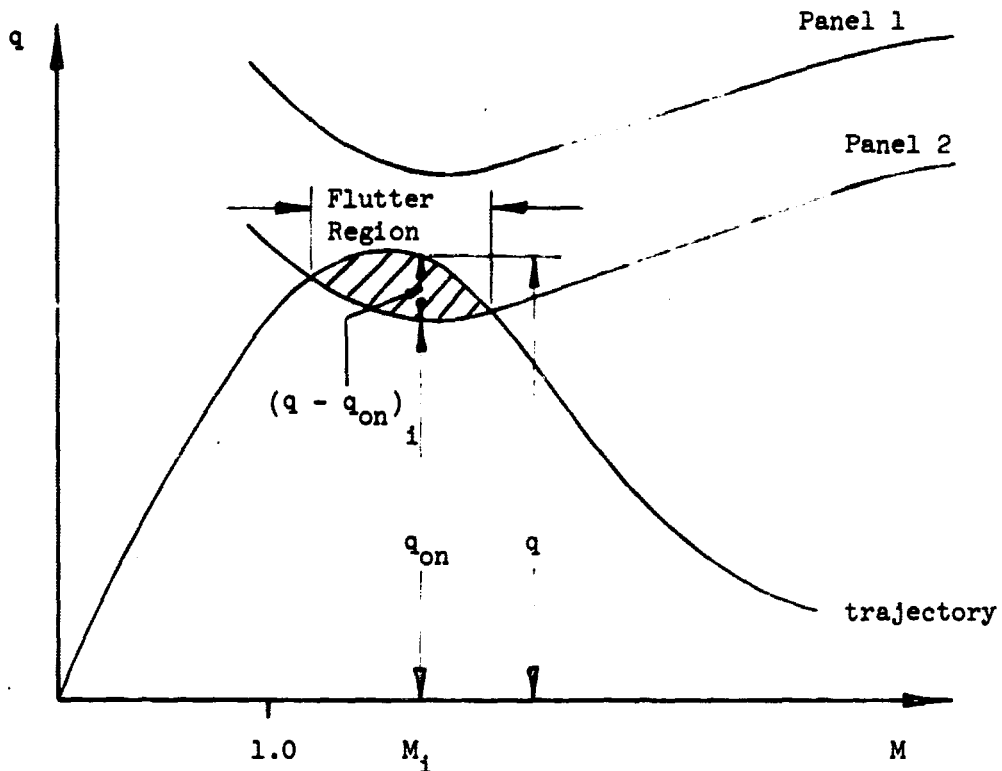
Step 2. Define Trajectory - Prepare trajectory information in the formats shown in the following sketches. For typical Saturn trajectories, maximum q occurs in the low supersonic region where panel flutter is most critical.



A factor of safety can be incorporated during the trajectory definition stage by increasing the trajectory dynamic pressure the desired percentage.

Step 3. Determine Flutter Onset - Determine flutter onset dynamic pressure q_0 at zero in-plane compressive load from Figure 1 for Mach range of trajectory. Calculate corresponding flutter onset dynamic pressure q_{on} at buckling by multiplying q_0 by the buckling correction factor given in Figure 2. Superimpose q_{on} so obtained on the M versus q plot. The following sketch typifies such plots for two panels. Panel 1 will not flutter throughout the flight trajectory and all such panels are dropped from further treatment. Panel 2 will flutter throughout that part of the trajectory corresponding to the

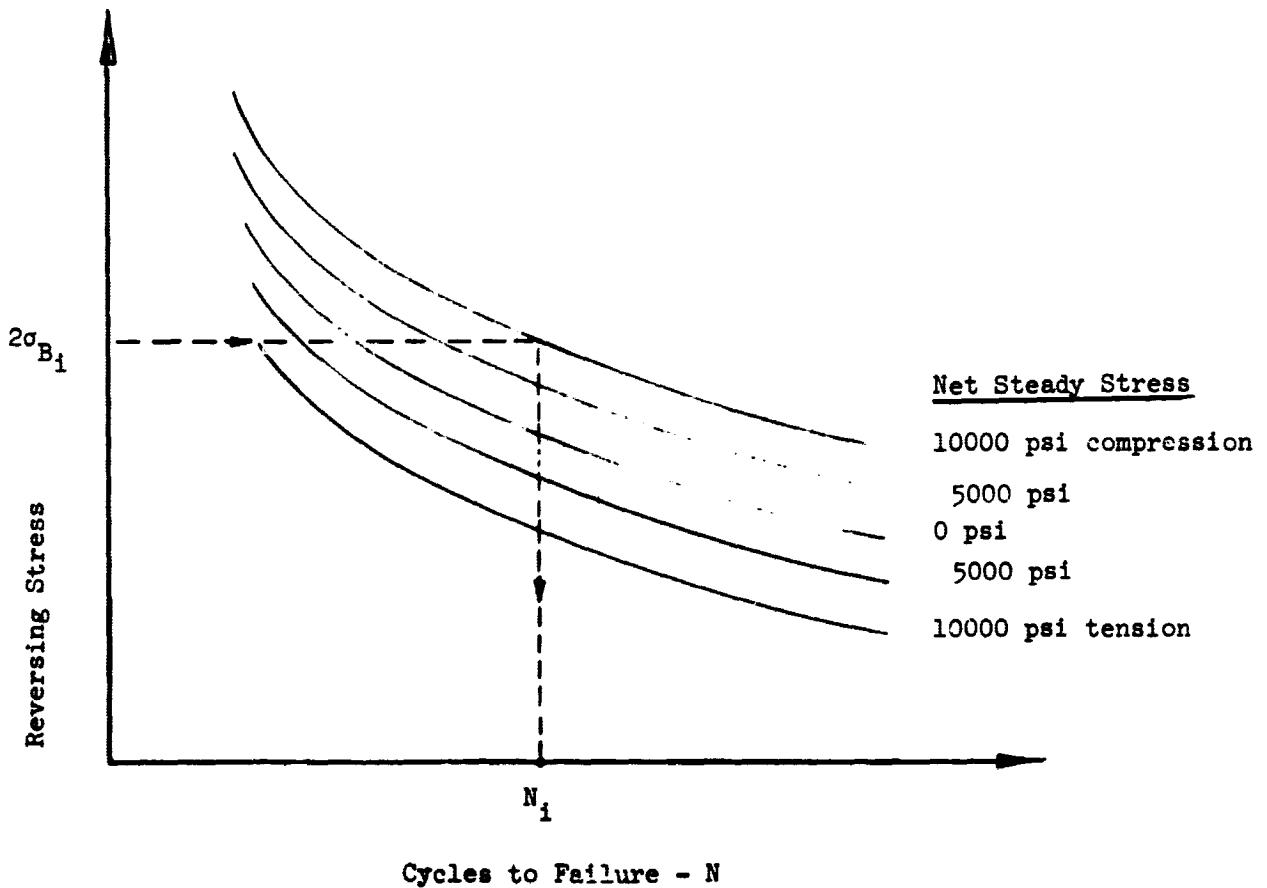
shaded area. Such panels require further study to assess whether or not fatigue failure will result.



Step 4. Panel Stresses at M_1 - It is convenient to consider the trajectory as a finite series of segments of constant M and constant q (see sketch in Step 2). Designate the Mach number M_1 . Then calculate the flutter penetration factor $\bar{q}_1 = \frac{(q_1 - q_{on_1}) W^4}{Dt}$ where the dynamic pressures are the trajec-

tory and buckled flutter onset values corresponding to M_1 . Enter the left hand portion of Figure 3 at the value corresponding to the penetration factor \bar{q}_1 and project upward to the L/W under consideration. This determines a non-dimensional surface stress parameter ($\bar{\sigma}$) needed in the expression for determining the total surface stress $\sigma_{max} [= \bar{\sigma} E (\frac{t}{W})^2 / (1-\nu^2)]$. This total surface stress (σ_{max}) is then resolved into its component bending stress (σ_B) and induced membrane stress (σ_M) by projecting to the right hand part of the chart and reading the stress percentages directly.

Step 5. Fatigue Damage at M_1 - From a fatigue standpoint, the peak to peak induced membrane (tensile) stress is treated as a steady stress (as explained elsewhere in this report). This should be combined with the applied compressive stress to arrive at a net steady stress for fatigue calculations. The bending stress alone is treated as the cyclical stress in the fatigue calculations (as explained elsewhere). Using a standard fatigue curve for the panel material under consideration, enter the curve after applying the desired stress concentration factor, at the net steady stress and twice the bending stress σ_B (since the reversing stress in fatigue curves is peak-to-peak rather than zero-to-peak as determined from Figure 3). See sketch below. Read off number of cycles to failure, N_1 .



The fatigue damage at the Mach number M_i is computed from

$$\Delta H = \frac{(\omega_f/\pi) \Delta t_i}{N_i}$$

where ω_f is the panel flutter frequency (rad/sec) determined from Figure 4 and Δt_i is the time at the Mach number M_i .

Step 6. Assess Panel Integrity During Trajectory - Repeat the procedure for the complete trajectory and form the sum

$$H = \sum \Delta H = \frac{\omega_f}{\pi} \sum \frac{\Delta t_i}{N_i}$$

If H is less than 1.0, panel will not fail; if greater than 1.0, failure will result.

3. DEVELOPMENT OF PREDICTION METHOD

Miner's Cumulative Damage Rule (Reference 4) is used to predict the fatigue life of fluttering skin panels. The rule is based on the value of the summation n/N where n represents the number of cycles at given mean stress and alternating stress levels and N represents the number of cycles to failure at those stress levels. The rule says that a fatigue failure can be expected if the summation exceeds 1.0. The Cumulative Damage Rule generally gives conservative predictions of fatigue life.

Application of this rule requires the following advance information:

1. The anticipated stress history during the structure service life (including both the mean and reversible stresses)
2. The number of cycles at each stress condition
3. The S-N plot of the structure material.

In terms of the panel flutter problem this first requires a means of predicting panel stresses as a function of dynamic pressure and Mach number. Obviously the prediction of these stresses is closely related to the prediction of flutter onset dynamic pressure since significant panel stresses (in the absence of excitation other than that due to airflow over the panel) occur only when the panel is fluttering; furthermore, onset dynamic pressure is needed as a reference for determining the depth of penetration into the flutter region. Once the stress during flutter is determined it must be represented in terms of alternating and mean stress components. The flutter frequency multiplied by the time duration at each panel M-q condition determines the number of stress cycles. Finally the material S-N plot is used to determine N at each corresponding stress condition. The sections below discuss each of these areas (prediction of flutter onset, stress during flutter, flutter frequency, and the material S-N plot) that are used to predict the fatigue life of Saturn V skin panels. The underlying assumptions are presented in Section 2.

3.1 Determination of the Flutter Onset Dynamic Pressure

The flutter onset criterion presented here is based on previously reported experimental flutter data (Reference 3, 5, 6, 7, 8). Theoretical trends were used to supplement available experimental data. The criterion is used to predict the buckled panel flutter onset dynamic pressure q_{on} for a panel with material modulus E , length L , width W and thickness t at a Mach number M . The flutter onset dynamic pressure is determined from the relation

$$q_{on} = F E \left(\frac{t}{L}\right)^3 K$$

where F and K are parameters discussed below.

The non-dimensional flutter parameter F is shown in Figure 1 as a function of Mach number with parametric variation in panel L/W and can be interpreted as the ratio of freestream dynamic pressure at flutter onset to panel stiffness for zero inplane edge load. The experimental points were obtained by introducing the experimental data into the equation given previously for F with K set equal to 1.0. The minimum value of F occurs between Mach 1.3 and 1.6 which implies that the minimum flutter onset dynamic pressure also occurs in this Mach number range. The values of F shown in the figure are conservative for the experimental data; that is, a q_{on} which is equal to or lower than the experimental flutter onset dynamic pressures will be predicted when using this criteria. The dotted extensions of the lines were extrapolated from the nearest experimental data by assuming that the flutter function increases with Mach number at the same rate as $\beta (= \sqrt{M^2 - 1})$. That is, if β increases 50% between two Mach numbers the extrapolated value of F increases 50% between the same two Mach numbers.

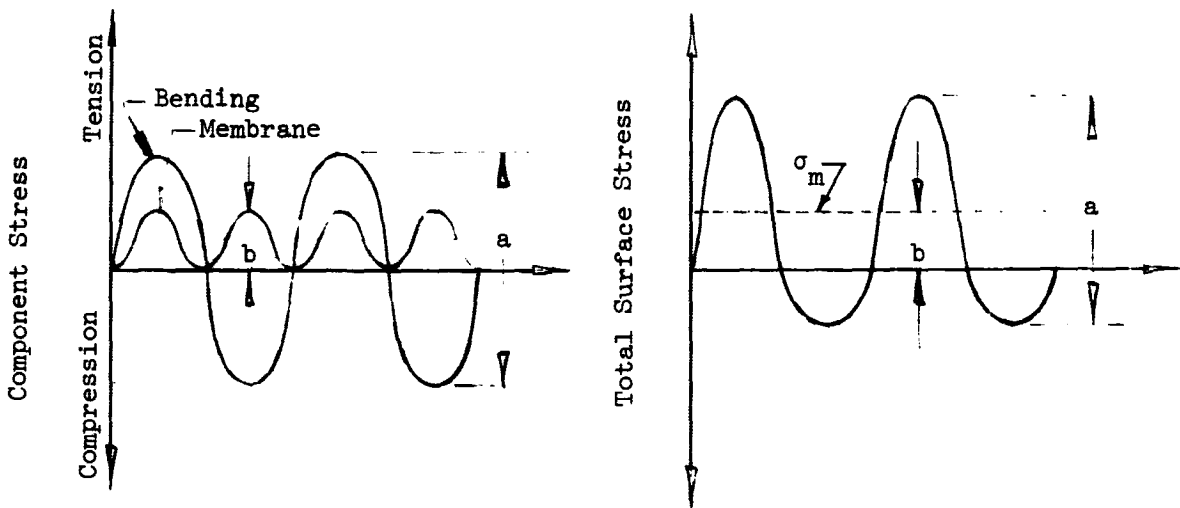
The buckling correction factor K accounts for the decrease in flutter onset dynamic pressure due to panel buckling. The value of K is equal to 1 when the panel is not compressively loaded. Figure 2 gives K as a function of panel L/W when the panel is loaded to the point of buckling. The scatter of the data plotted on Figure 2 necessitated a heuristic approach to determine the variation of K with L/W. The Reference 3 data was favored over the Reference 6 data for L/W's in excess of 3.0 because of the better repeatability of the flutter onset points.

3.2 Prediction of Stresses During Flutter

The maximum surface stress during flutter is shown in non-dimensional form in Figure 3a as a function of flutter penetration factor \bar{q} with parametric variation in panel L/W. This plot was obtained by combining experimental data with theoretical data given in Reference 9. Using the L/W = 4.48 flutter penetration data of Reference 3 as a firm base, curves for the other values of L/W were determined by employing theoretical trends given in Reference 9.

The experimental data given in Reference 3 was obtained from the flutter test of a single panel geometry: L = 30 inches, W = 6.7 inches, t = .032 inches. Stress data as a function of dynamic pressure (q exceeding q_{on}) was

given for the test panels when they were subjected to an inplane compressive edge load equal to 96% of buckling. Since Reference 3 does not give surface stress directly, it was necessary to "synthesize" a surface stress from the given values of induced axial and bending stress. During flutter the axial and bending stresses vary with time roughly as shown in the sketches below. The bending stress alternately takes on equal compressive and tensile values



while the induced axial (membrane) stress is always tensile and varies at twice the bending stress frequency. Thus the maximum surface stress (neglecting static inplane applied stress) is equal to the sum of one-half of the peak-to-peak bending stress ($a/2$) and the peak-to-peak axial stress (b). Notice that the peak-to-peak surface stress is equal to the peak-to-peak bending stress (a). The maximum surface stress, so synthesized, is shown in Figure 5 along with the experimental bending and axial stresses used in

the synthesis. It is replotted in Figure 6 in the non-dimensional format of Figure 3a. Figure 6 is actually the base curve of Figure 3a. The following paragraphs present details of the theoretical approach for determining the curves for other values of L/W.

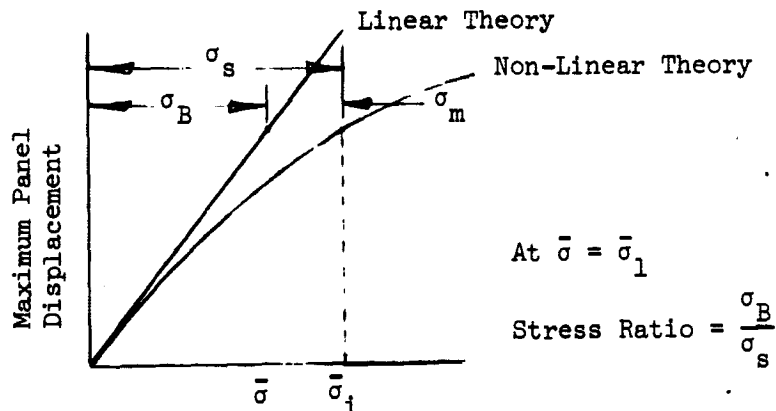
The theoretical stress data resulting from a non-linear analysis of clamped panels under a uniform static pressure is given in Figure 7. The dotted lines show linear analysis data. As can be seen in the figure, one value of the static pressure parameter (\bar{P}) results in different surface stresses depending on the panel L/W. As a first step in arriving at a relationship between the panel stresses occurring during flutter and those occurring under static differential pressure, a curve approximating L/W = 4.48 is sketched on Figure 7 between the L/W = 2 and L/W = 0 lines. Correspondence between \bar{P} and \bar{q} can be established by matching the experimental L/W = 4.48 data from Figure 6 with sketched 4.48 data on Figure 7. The flutter penetration parameter \bar{q} is just \bar{P} with the static pressure differential replaced by the dynamic pressure increment $q - q_{on}$. When values of \bar{q} have been established for several values of \bar{P} on Figure 7, the figure can be used to determine $\bar{\sigma}$ as a function of \bar{q} for values of L/W other than 4.48. Two assumptions made for the extrapolation procedure are:

1. Measured surface stresses were maximum (measured near panel trailing edge)
2. The ratio of $\bar{\sigma}$'s for different L/W at constant \bar{P} (Figure 7) establishes the ratio of $\bar{\sigma}$'s for different L/W at a constant \bar{q} (Figure 3a)

The latter assumption establishes the variation with L/W of maximum surface stress during flutter.

Figure 3a allows the total surface stress to be determined for any \bar{q} . This total surface stress must be separated into its axial and bending stress components for estimating the fatigue life. Since Reference 9 also includes linear analysis data, i.e. bending stresses only, which are directly proportional to the panel displacement, the ratio of bending stress to total stress can be calculated as a function of $\bar{\sigma}$ for the different L/W's. The theoretical data from Reference 9 can be plotted to show panel displacement as a function of surface stress. Thus at any panel deflection the ratio of bending stress to surface stress (surface stress is equal to membrane or axial plus bending stress) can be obtained by dividing the linear theory surface

stress by the non-linear theory surface stress (See sketch).



This stress ratio is then plotted as a function of total surface stress as shown in Figure 3b.

3.3 Estimation of Flutter Frequency

The flutter frequency is estimated by solving the equation:

$$\omega_f = \left\{ \frac{\Omega D}{tL^3 W} \right\}^{1/2}$$

The non-dimensional flutter frequency parameter Ω , which is a function of L/W , was determined from experimental flutter frequencies using the above equation. (See Figure 4). This formulation of the frequency parallels the development presented in Reference 10 for prediction of "still air" natural frequencies. The current application of the frequency equation replaces an analytical expression given for Ω in Reference 10 with an empirical function of L/W based on experimental flutter frequency data. This flutter frequency calculation procedure assumes that the frequency is independent of Mach number, dynamic pressure, and compressive edge load.

The stress frequency can deviate from the flutter frequency as noted in Reference 3. This reference pointed out that during flutter the response amplitude of the downstream half of a buckled panel was dominated by the first harmonic component of the flutter frequency. To account for this odd behavior it was assumed in the fatigue criterion that the stress frequency was twice the fundamental flutter frequency.

3.4 S-N Diagram

The S-N diagram for 7075-T6 aluminum is shown in Figure 8. As is expected the number of cycles to fatigue failure increases as the alternating stress decreases; in addition, the fatigue life increases when the mean stress

is compressive and decreases when the mean stress is tensile. In this application the alternating stress is the peak-to-peak bending stress as discussed in Section 3.2. The mean steady state stress is the peak-to-peak induced membrane stress combined with applied compressive stresses.

Before entering the S-N diagram at a given stress condition, an appropriate stress concentration factor is applied to both the alternating and mean stresses to account for the effects of rivet hole size and layout along the panel edges. Reference 11 develops a technique for calculating stress concentration factors. Detail of the fatigue life calculation using Miner's rule is presented in Section 2.

3.5 Conservatism

Conservatism has been incorporated in this fatigue prediction procedure in several respects, namely:

- o The method used to predict onset dynamic pressure is known to be conservative to account for uncertainties in panel and/or flow characteristics.
- o Although boundary layer thickness is known to be stabilizing (Reference 14), the boundary layer thickness on the Saturn vehicle is neglected.
- o Differential pressure across the panels is assumed to be zero even though it is anticipated that non-zero pressures (strongly stabilizing, see Reference 3) will exist during portions of the trajectory.
- o It is generally accepted that the Miner's cumulative fatigue criterion is conservative.

While it would be virtually impossible to establish a degree of conservatism for the procedure, an experimental case has been checked. An aluminum panel described in Reference 3 did not fail after fluttering for 20 minutes. The present criterion predicted a fatigue life of less than 5 minutes for that panel. As with all criteria, the judgment of the user provides the ultimate assessment of results.

4. APPLICATION OF PROCEDURE TO SATURN V PANELS

The procedure described in Section 3 is applied in this section to assess the flutter integrity of skin panels on the Saturn S-V launch vehicles. The procedure was to first determine the panels that were flutter susceptible and then to estimate the fatigue life of those panels.

4.1 Criterion Input Information

4.1.1 Launch Trajectory - The Saturn/Apollo lunar trajectory (Figure 9) is more critical from a panel flutter standpoint than other S-V trajectories and was used in this study. The trajectory dynamic pressures were increased by 33% in keeping with NASA design procedures. (The trajectory was subdivided into 49 one-tenth Mach number increments between Mach 1.0 and Mach 5.0. Computations were made at each of the 49 Mach numbers using the appropriate trajectory time interval and dynamic pressure. The range time elapsing between Mach 1.0 and 5.0 is 52 seconds).

4.1.2 Panel Material Properties - The Saturn V skin panels are all 7075-T6 sheet. The important properties of this alloy are:

| | | |
|-----------------|--------------|--|
| Young's Modulus | Tension: | 10,300,000 psi |
| | Compression: | 10,500,000 psi |
| Poisson's Ratio | | .35 |
| Density | | .101 pounds/in ³ |
| Yield Stress | | 66,000 psi |
| Endurance Limit | | 20,000 psi alternating stress for zero mean stress but varies with mean stress |

The S/N plot given in Figure 8 was used to determine fatigue damage at each M-q condition.

4.1.3 Panel Geometries - Table I presents typical S-V skin panel geometries. (The W = 6.7 inch panel selected for the investigation of Reference 3 provides an upper limit in width and also a basis for extrapolating stress prediction to other panels.) Panel thicknesses of greater than .065 inches are not flutter susceptible in the lunar trajectory; only the .03, .032, and .04 gauge skin panels are flutter susceptible. Thirty-five panels each 6.7 inches wide with lengths of 6.7, 13.4, 20.1, 26.8, 33.5 inches (L/W = 1,2,3,4,5) and thicknesses of .02, .025, .03, .032, .04, .05, .055 inches, were chosen as the basis of the study. Additional panels with widths

22 February 1971

other than 6.7 inches were also studied to determine the effects on fatigue of altering the panel width. The selected geometries cover a large range of panels and the conclusions concerning these panel geometries should extend to all susceptible panels on the Saturn vehicle.

4.1.4 Stress Concentration Factor - A stress concentration factor of 3.0 was used in all stress calculations. Data presented in Reference 11 was used to establish the stress factor for typical Saturn panel rivet hole layouts.

4.2 Results

4.2.1 Flutter Penetration - The maximum calculated dynamic pressure penetration (Λ) during the launch trajectory is shown in Figure 10 as a function of panel L/W and thickness for unloaded and buckled panels. When Λ is equal to 1.0 the panel just begins to flutter. Maximum penetration occurs for buckled panels having length width ratios of 2 and 3. The duration of flutter for the panel geometries examined is shown in Figure 11. As indicated on the figure some of the panels with thicknesses less than .03 inches were still fluttering at Mach 5.0. However, the stresses occurring during this high Mach number flutter were always less than the endurance limit so that the panel fatigue life would not be affected. (The flutter parameter F for L/W = 5.00 was obtained by direct extrapolation from the values given on Figure 1 for L/W = 3.0 and 4.0.)

4.2.2 Maximum Alternating Stress - The maximum predicted alternating stress (peak-to-peak bending stress) was about 38,000 psi obtained for the L/W = 2.0 and 3.0 panels when the thickness was .05 inch. Alternating stress data for the different panel geometries is shown on Figure 12. The data for panels thinner than .03 inch is somewhat questionable because the penetration parameter \bar{q} for these panels was far in excess of the experimental \bar{q} range (< 8,000) represented by the data given in Reference 3. A linear extrapolation of data shown on Figure 3a was assumed for values of \bar{q} in excess of 8,000. It is interesting to note that maximum stress and maximum flutter penetration do not coincide. This is because the alternating stress is proportional to the product of $\bar{\sigma}$ and the thickness squared. The decrease in $\bar{\sigma}$ due to increase in panel thickness is not sufficient to offset the thickness squared term.

4.2.3 Flutter Frequency - The calculated panel flutter frequencies are plotted in Figure 13 as a function of panel thickness and L/W. For constant L/W the criterion assumes on the basis of panel natural frequency trends, that the flutter frequency increases linearly with panel thickness.

4.2.4 Panel Fatigue Life - The S-N plot for 7075-T6 aluminum presented earlier (see Figure 8) was used to predict panel fatigue life. Failure cycle data was obtained by entering the plot at the calculated alternating stress and mean stress (mean stress within $\pm 5,000$ psi of the nearest 10,000 psi contour). No fatigue failure was predicted for any of the panels studied. The final values of the Miner's fatigue summation ($\sum n/N$) are given in Figure 14. The trend closely resembles that found for the maximum alternating stresses. The greatest fatigue damage estimated, which was about 20% of failure, was for a panel with L/W of 2 and thickness of .05 inches.

4.2.5 Effect of Changing Panel Width - Decreasing the panel width from 6.7 inches while holding L/W and thickness constant reduces fatigue damage since the flutter onset dynamic pressure increases. Increasing the width from 6.7 inches reduces the maximum panel stress even though the flutter penetration is increased. The reduction in stress occurs because stress varies as $\bar{\sigma}$ divided by the width squared. When the width is increased, the squared term increases faster than $\bar{\sigma}$. The result of a lower maximum stress is less fatigue damage. The maximum alternating stresses and fatigue damage summations can be compared in Table 1 for the different width geometries checked.

4.3 Conclusion

This application of the flutter fatigue criterion indicates that no skin panel fatigue failure will occur on the Saturn V launch vehicle for trajectories comparable to the Apollo lunar trajectory. The analysis further indicates that the panels could survive at least 5 missions without danger of fatigue failure (note that the inverse of the failure index $\sum n/N$ represents the number of missions before failure). Thus in terms of a single mission, the Saturn panels have at least a 400% margin of fatigue safety.

A stress factor of safety is defined for the Saturn as the ratio of the maximum calculated alternating stress during the trajectory to a reference failure stress. The reference failure stress is defined as the constant alternating stress required to cause failure within the critical 52 second

flight period. Figure 15 presents plots of the stress factor of safety versus thickness for values of L/W between 1 and 5. When this factor exceeds one, the possibility of fatigue failure demands closer investigation. The largest value for the S-V panels was .73 for a panel with L/W = 2 and a thickness of about .045 inch.

Table I - Geometry of Representative Panels on the S-V, S-IB Vehicles

| Location | L(inches) | L/W | t (inches) |
|-----------------------|------------|-----------|------------|
| S-IVB Fwd Skirt | 3.12-30.6 | .96-5.12 | .032 |
| S-IVB Aft Skirt | 8.34-18.3 | 2.98-6.54 | .04 |
| S-IVB/S-II Interstage | 14.4-29.0 | 2.5-8.8 | .04 |
| S-II Fwd Skirt | 22.0-33.9 | 6.3-17.8 | .03-.04 |
| S-II Aft Skirt | 12.0-36.2 | 5.13-15.5 | .071 |
| S-II/S-IC Interstage | 17.86-38.5 | 7.7-16.5 | .071 |
| S-1C Fwd Skirt | 32.0-36.0 | 14.7-16.6 | .10 |
| S-1C Aft Skirt | 24.0-31.0 | 6.4-8.3 | .2-.45 |

This data is taken from Reference 13

Table II - Effect of Change Panel Width

L/W = 2.0

| | σ_{max} (psi) | | | | | | $\Sigma n/N$ | | | | |
|-------------------------|-----------------------------|--------|--------|--------|--------|------|--------------|-----|-----|-------|--|
| | 3.0 | 5.0 | 6.7 | 8.0 | 10.05 | 3.0 | 5.0 | 6.7 | 8.0 | 10.05 | |
| Width \longrightarrow | 3.0 | 5.0 | 6.7 | 8.0 | 10.05 | 3.0 | 5.0 | 6.7 | 8.0 | 10.05 | |
| Thickness = .045 | N.F. | 26,849 | 36,641 | 34,485 | 28,725 | N.F. | .0025 | .17 | .13 | .028 | |
| Thickness = .050 | N.F. | N.F. | 37,384 | 36,489 | 30,636 | N.F. | N.F. | .16 | .15 | .05 | |

N.F. - No Flutter in Trajectory

$$F = \frac{q_0}{E} \left\{ \frac{L}{t} \right\}^3$$

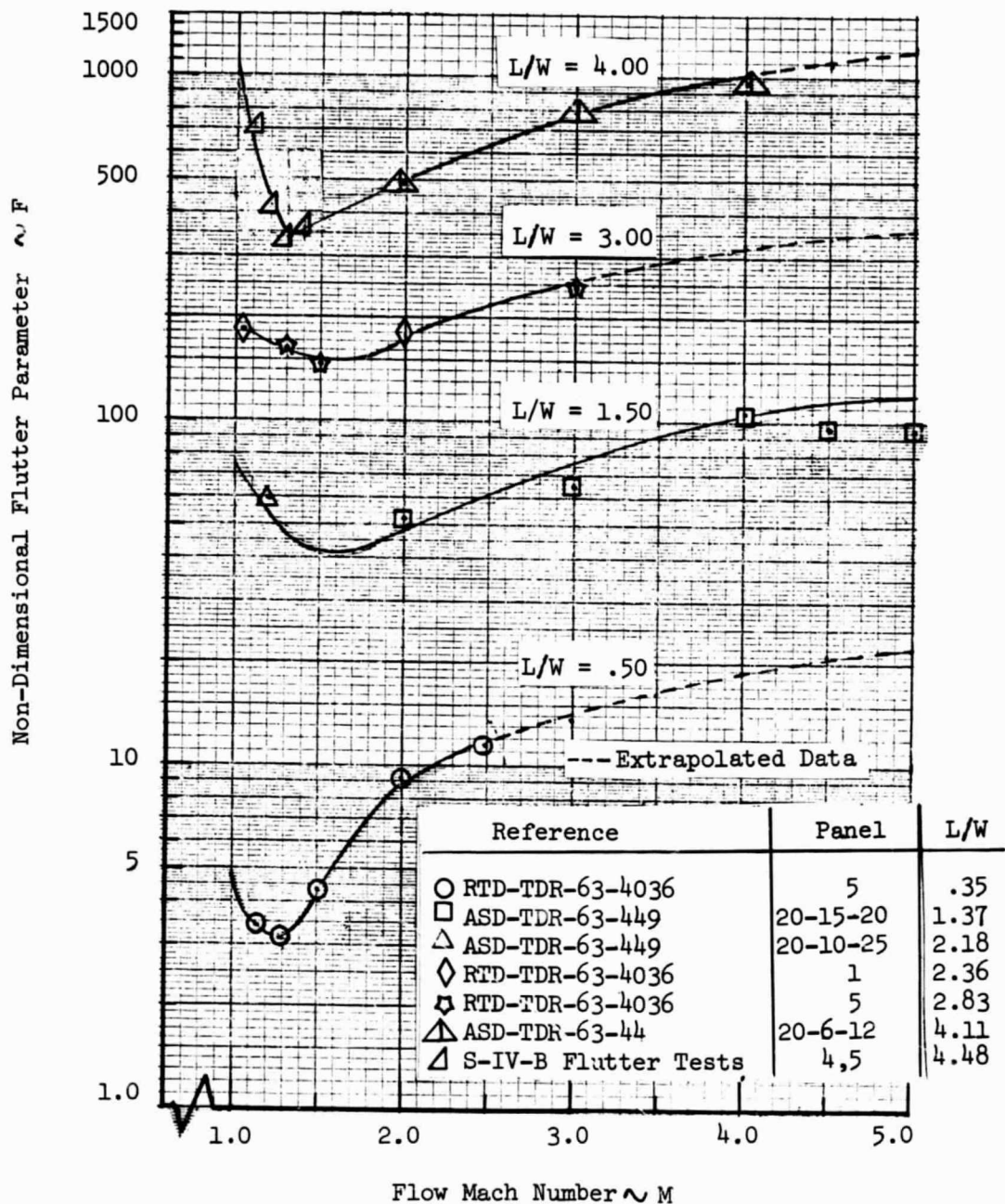


Figure 1 - Non Dimensional Flutter Parameter Versus Flow Mach Number

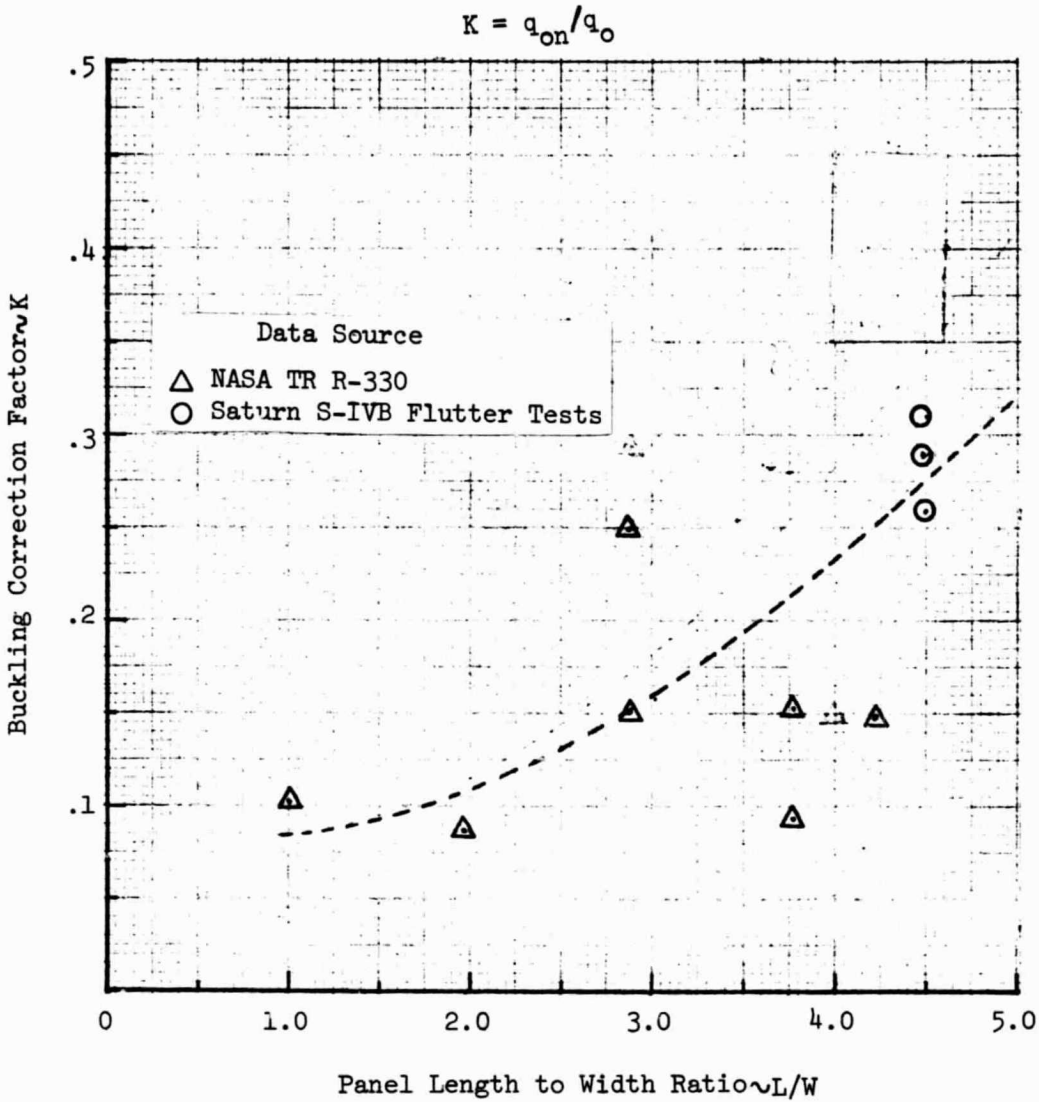


Figure 2 - Correction to Account for Lowering of Onset Dynamic Pressure due to Panel Buckling

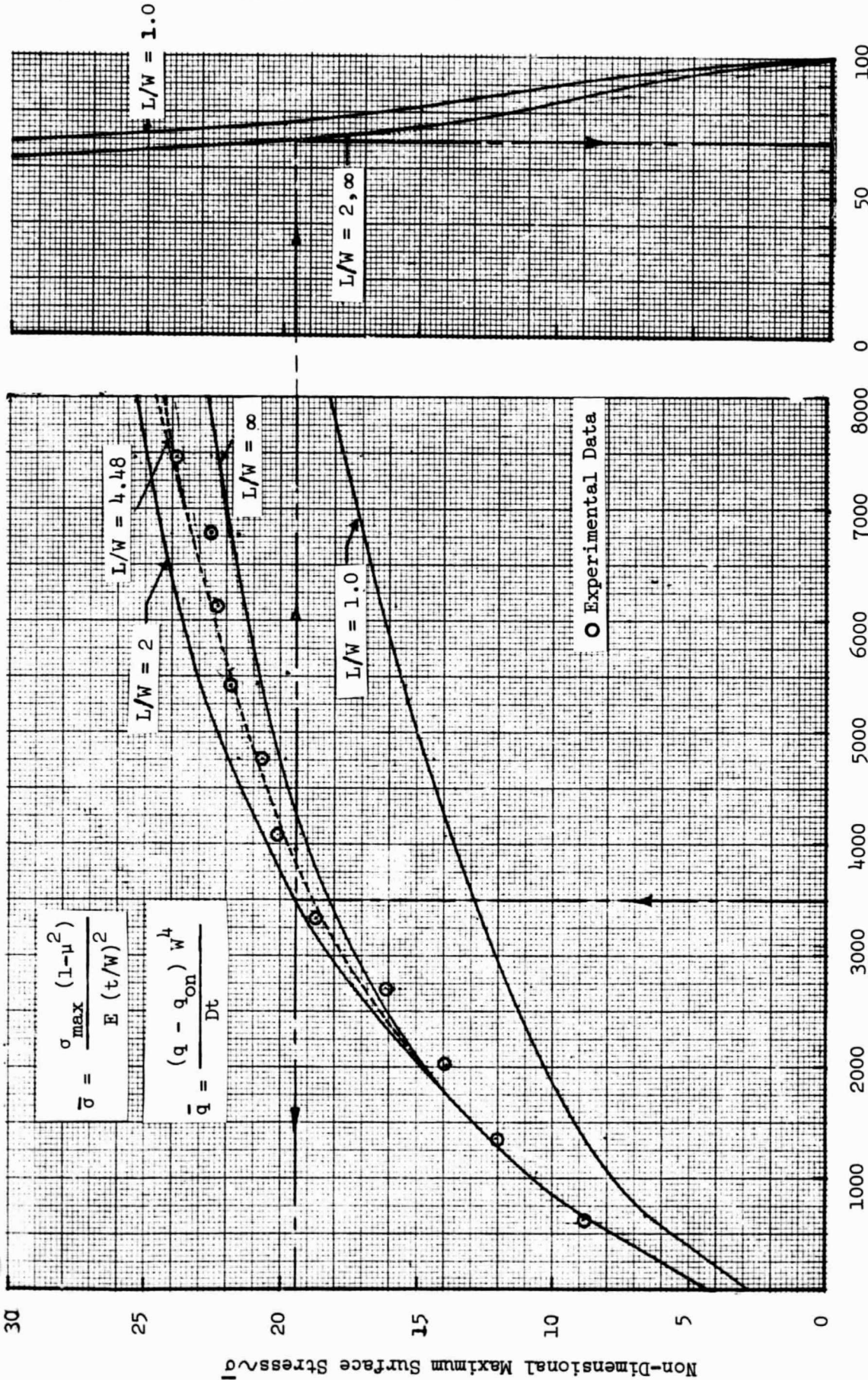


Figure 3a Non-Dimensional Surface Stress as a Function of Flutter Penetration Factor

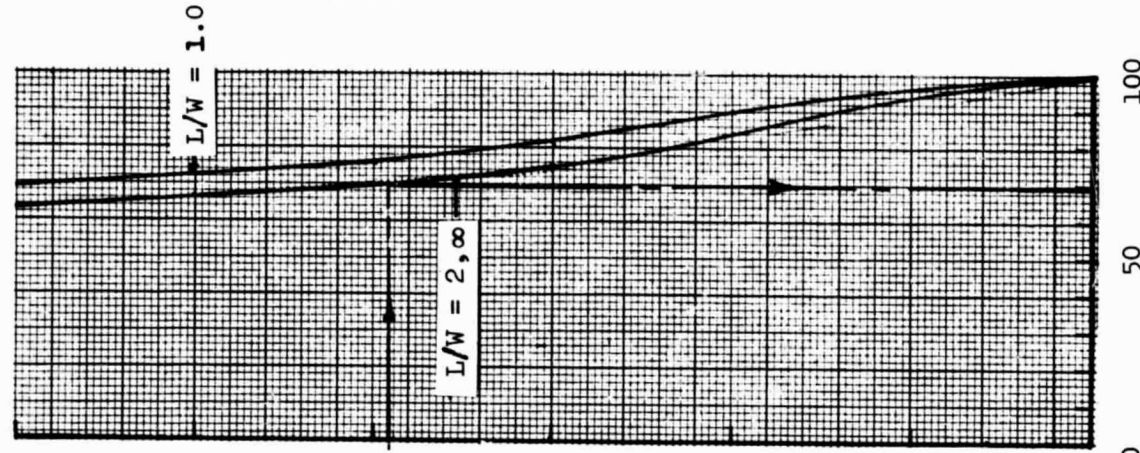


Figure 3b Percentage of σ_{\max} due to Bending Stress

Symbols

- Saturn S-IVB Tests
- △ TR R-330, Panel 5
- RTD-TDR-63-4036, Panel 1
- ▴ RTD-TDR-63-4036, Panel 5
- ☆ ASD-TDR-63-449, Panel 10-20-12
- ASD-TDR-63-449, Panel 20-15-20
- ◇ TR R-330, Panel 2
- ◇ RTD-TDR-63-4036, Panel 1
- ASD-TDR-63-449; Panel 20-6-12

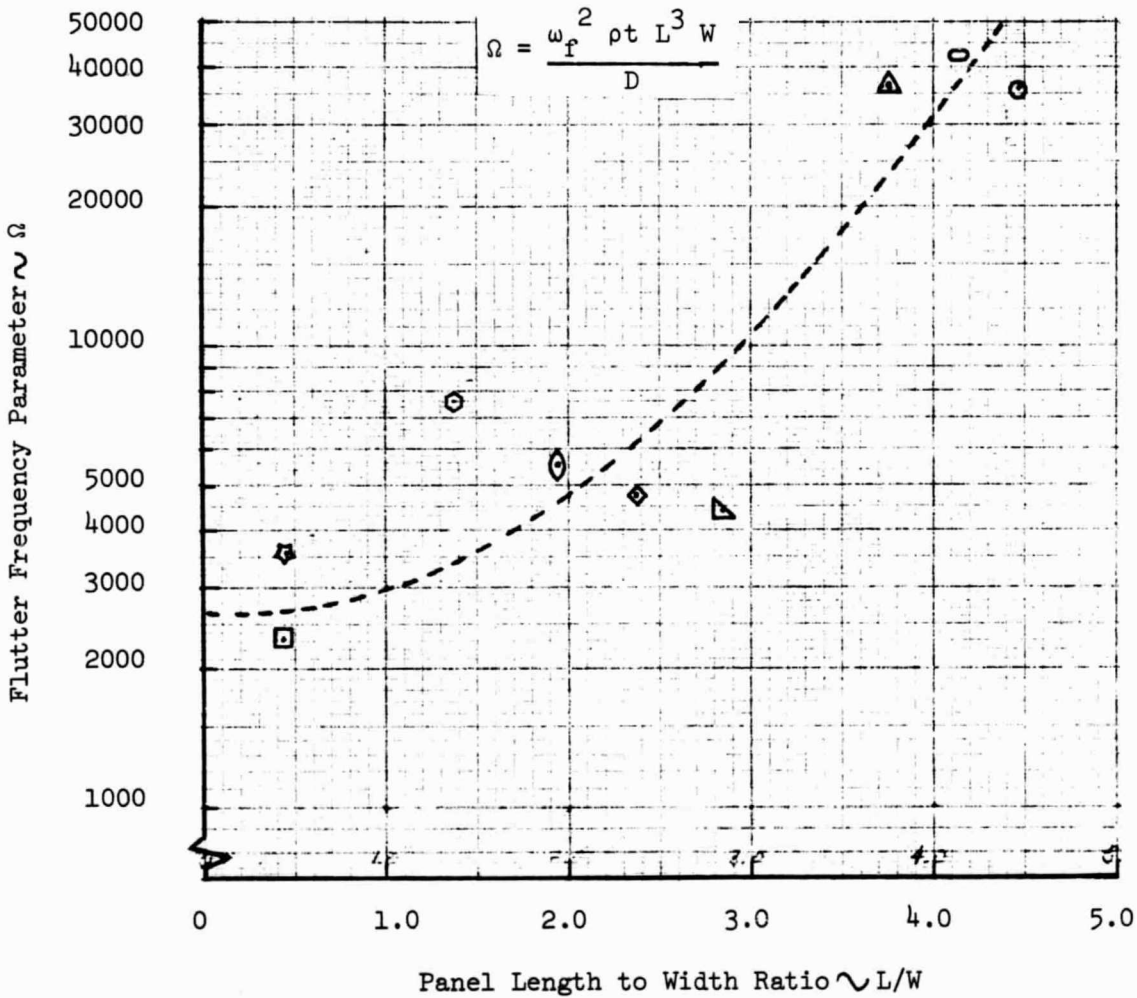
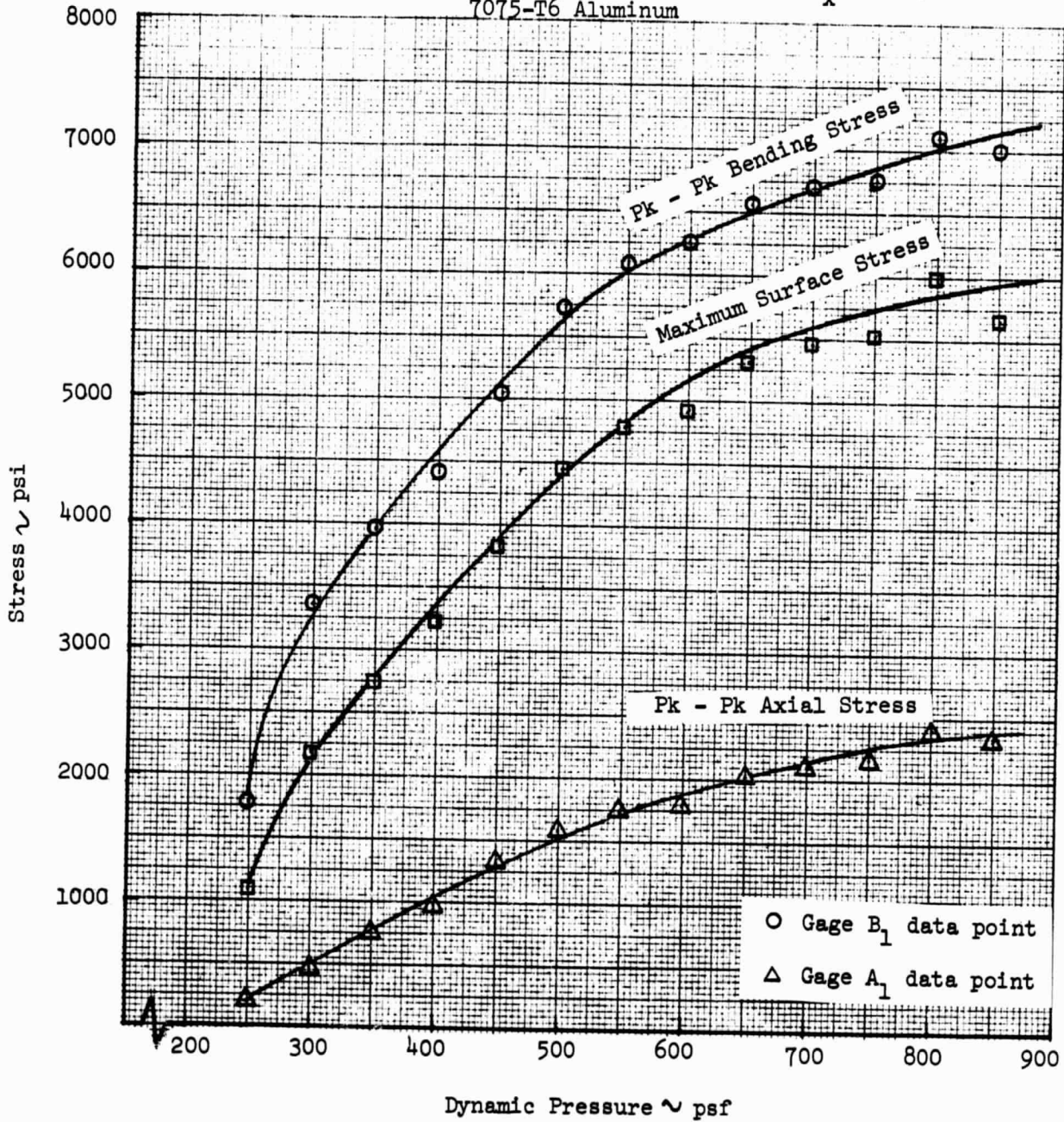


Figure 4 Experimental Flutter Frequency Parameter Versus L/W

$L/W = 4.48$, $W = 6.7$ inches, $t = .032$ inches, $N_x = .96$, $M = 1.3$
7075-T6 Aluminum



Data adapted from
Reference 3

Figure 5 Stress as a Function of Dynamic Pressure

$$\bar{\sigma} = \frac{\sigma_{\max} (1 - \mu^2)}{E (t/w)^2}$$

$$\bar{q} = \frac{(q - q_{on}) w^4}{Dt}$$

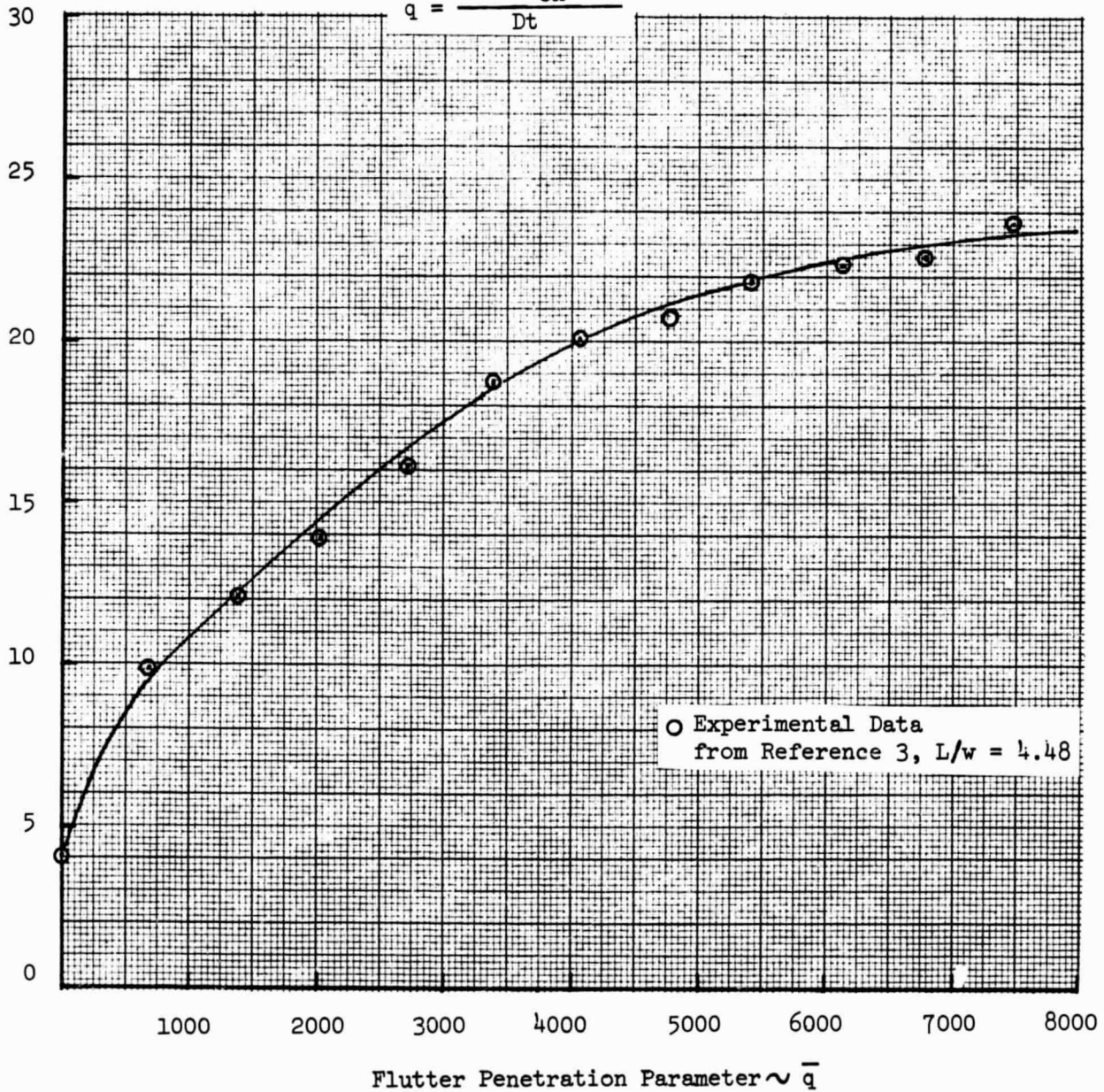


Figure 6 Non-Dimensional Surface Stress as a Function of the Flutter Penetration Parameter

$$\bar{\sigma} = \frac{\sigma_{\max} (1 - \nu^2)}{E (t/W)^2}$$

$$\bar{P} = \frac{\Delta P W^4}{Dt}$$

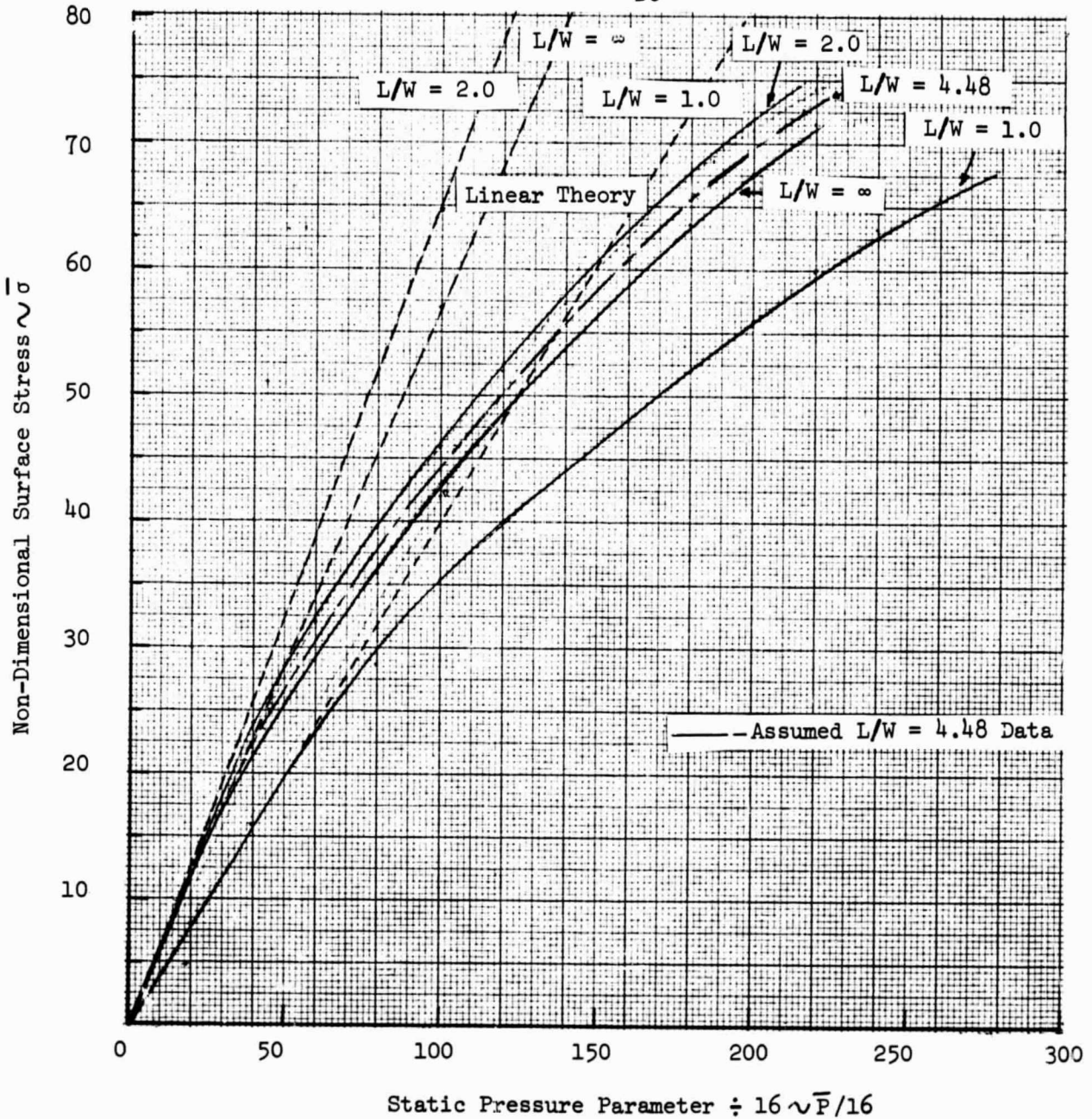
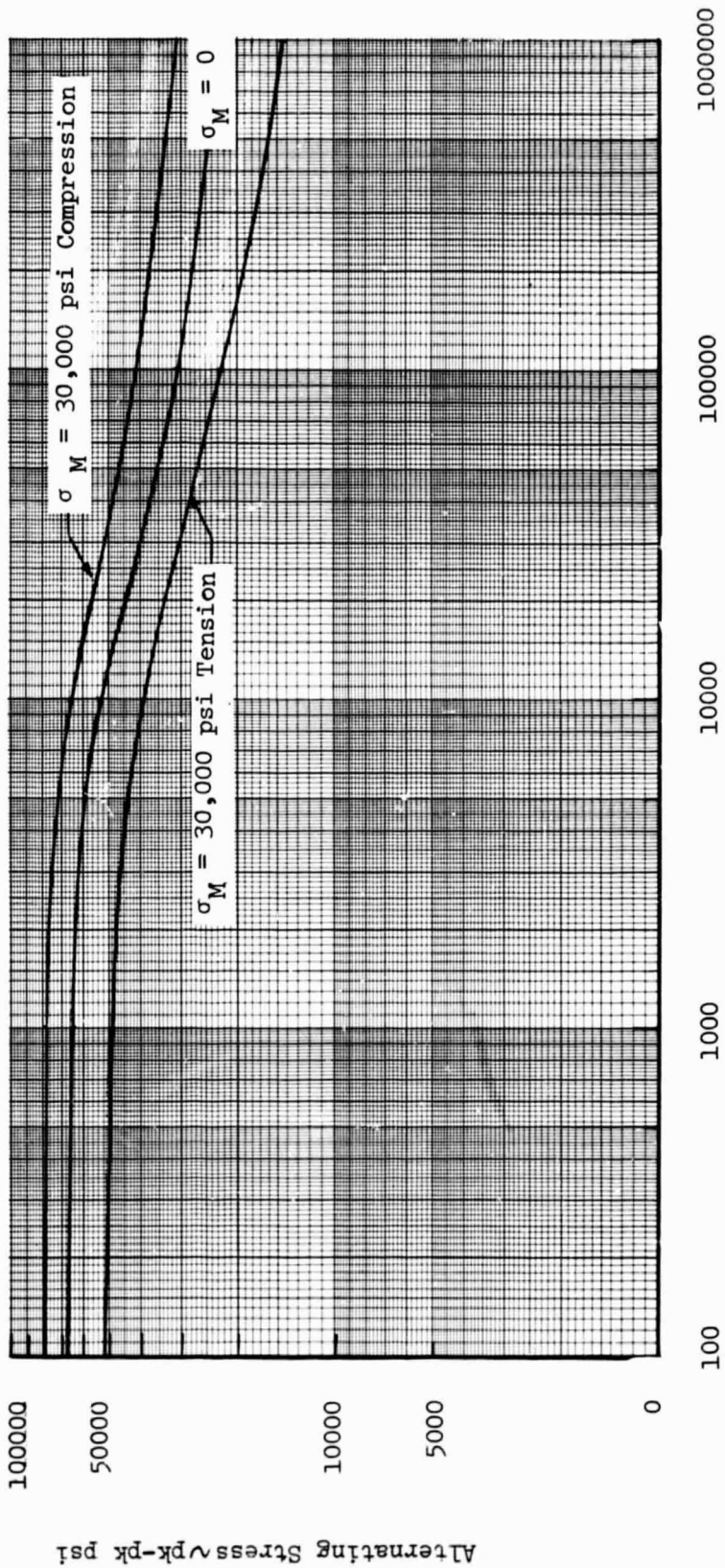


Figure 7 Theoretical Non-Dimensional Surface Stress Variation with Static Pressure Parameter



Data shown was taken from
Reference 12

Oscillation Cycles to Failure ~ Hz

Figure 8 S-N Diagram for 7075-T6 Aluminum Sheet

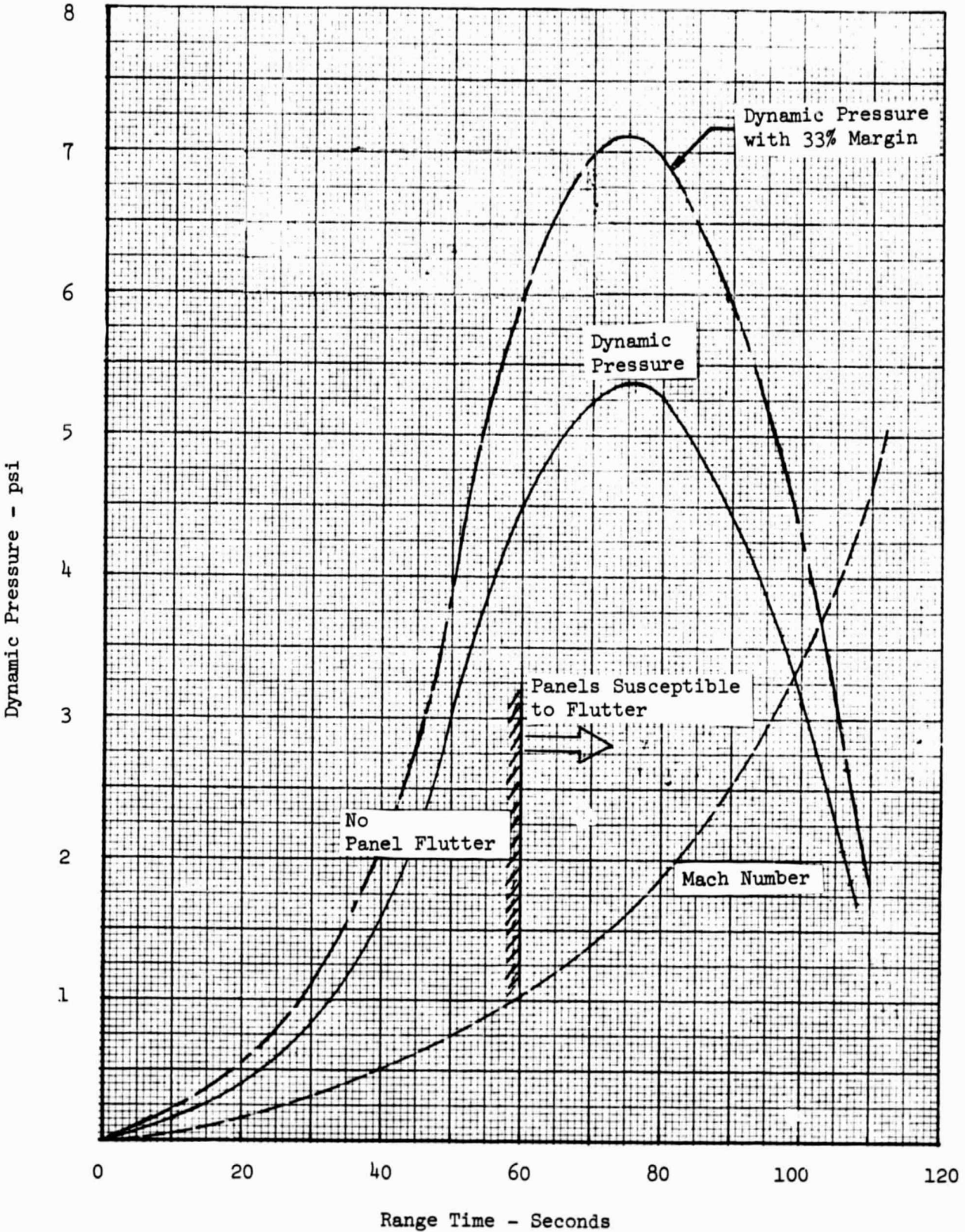


Figure 9 - Apollo/Lunar Trajectory

Panel Width = 6.7 inches

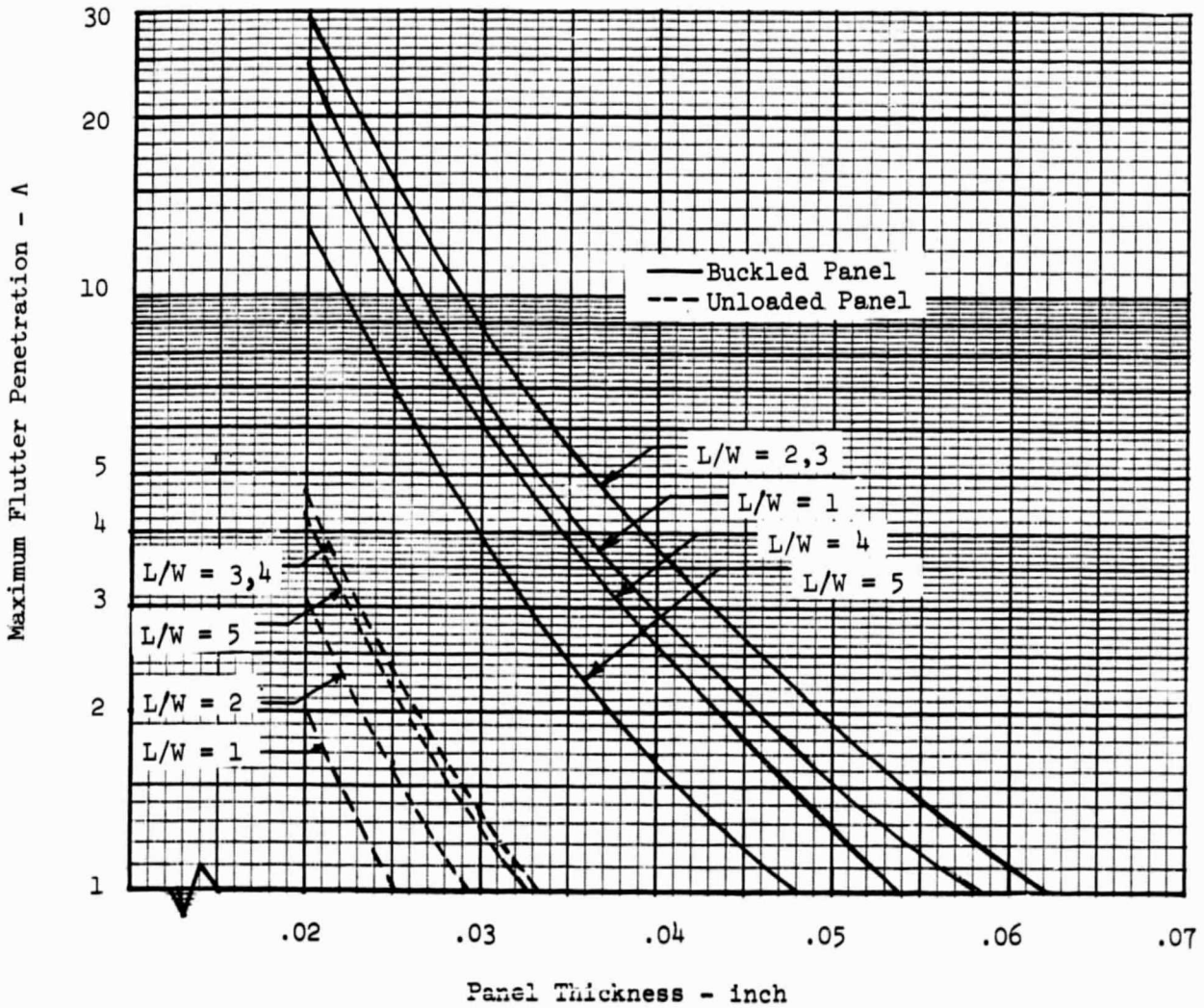


Figure 10 - Maximum Flutter Penetration as a Function of Panel Geometry

Panel Width = 6.7 inches

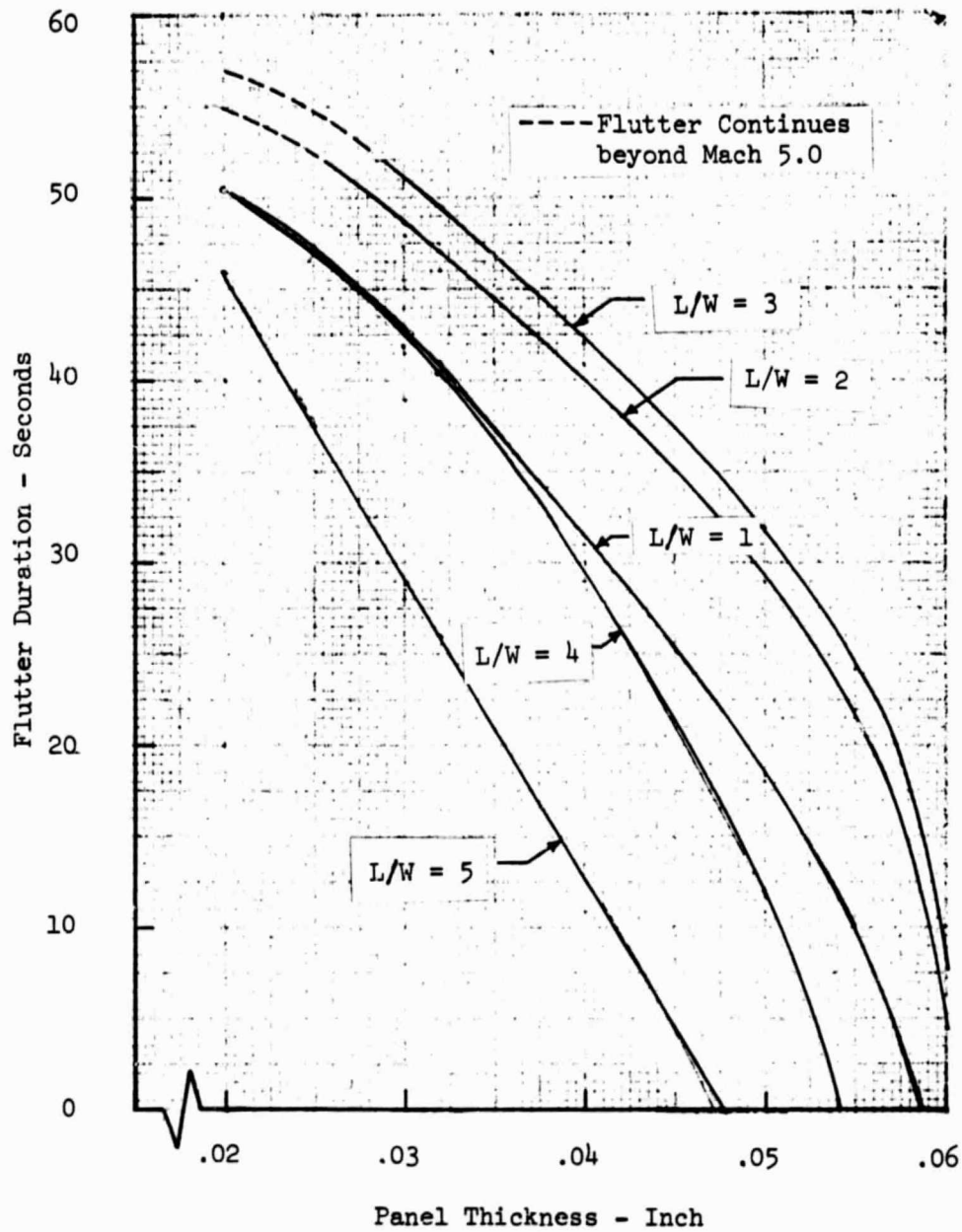


Figure 11 - Flutter Duration as a Function of Panel Geometry

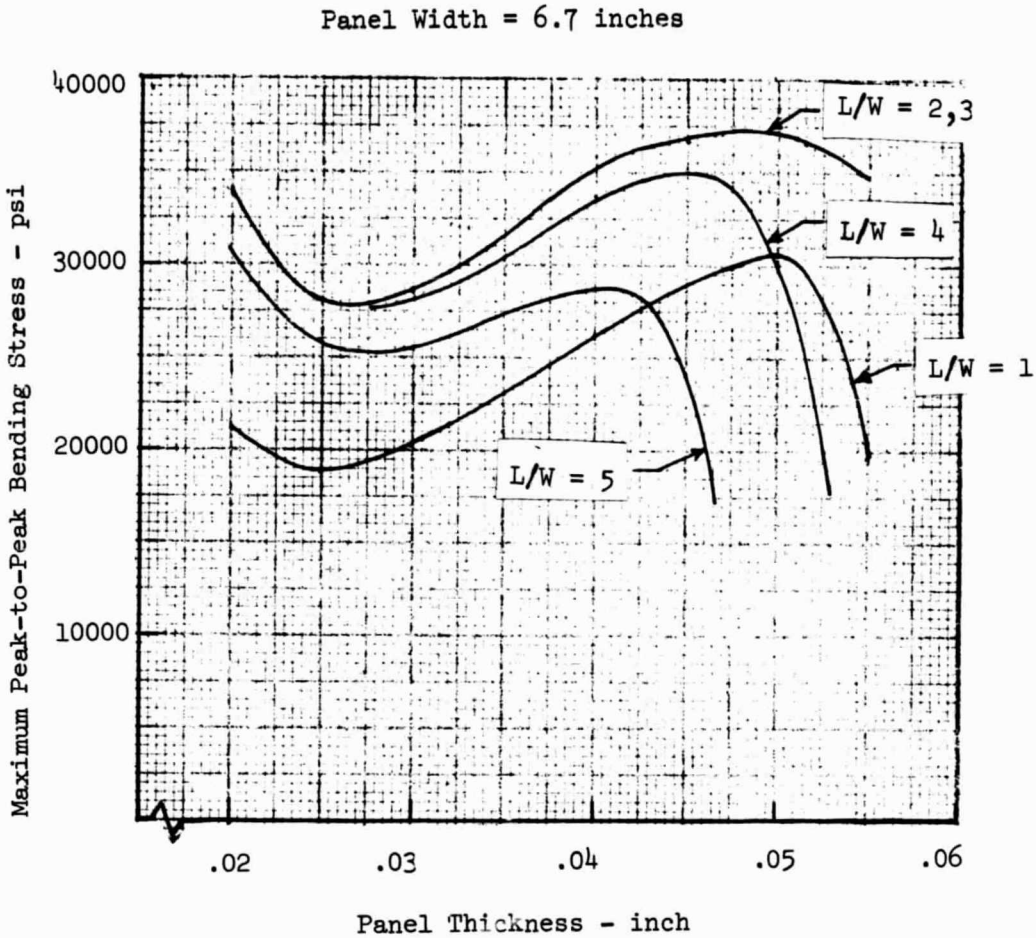


Figure 12 - Maximum Bending Stress as a Function of Panel Geometry

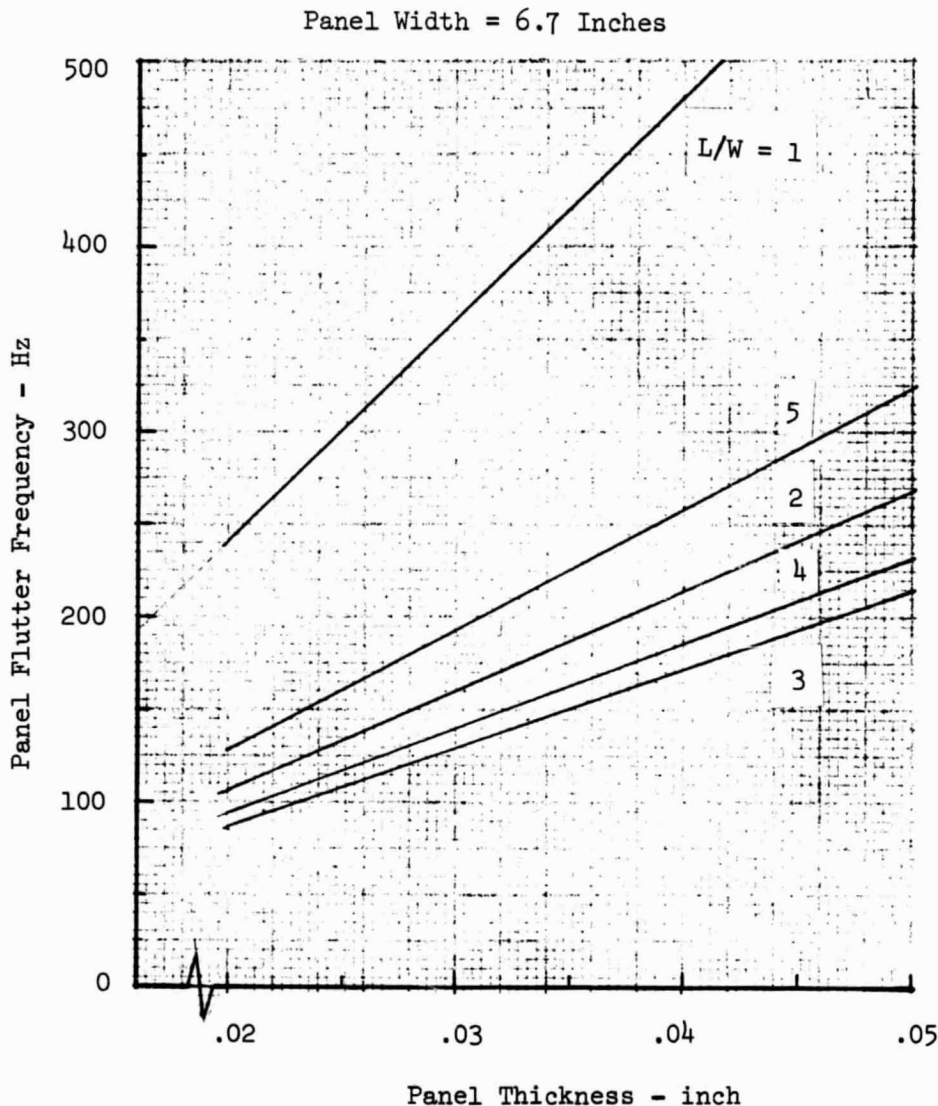


Figure 13 - Flutter Frequency as a Function of Panel Geometry

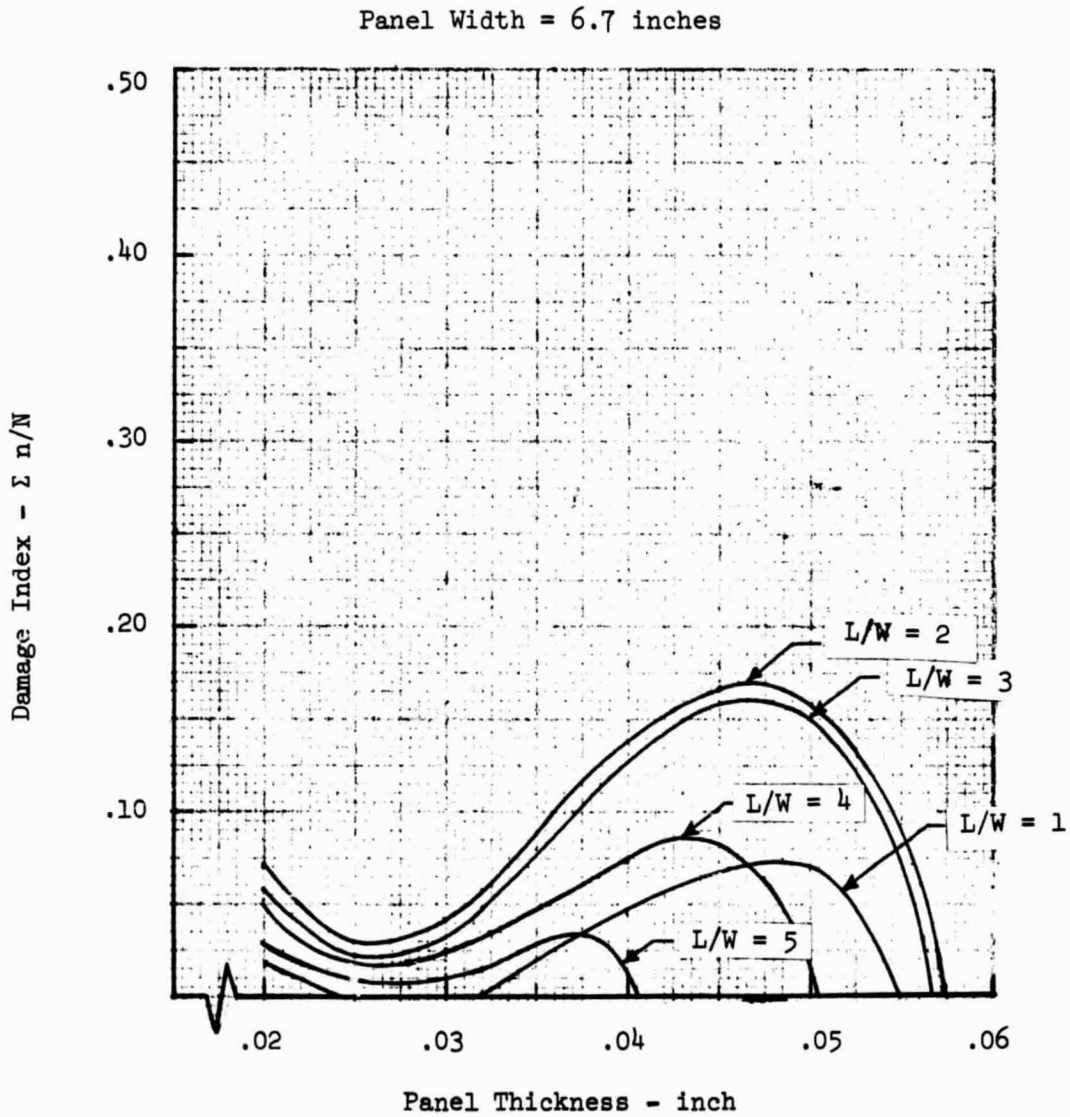


Figure 14 - Miner's Damage Index as a Function of Panel Geometry

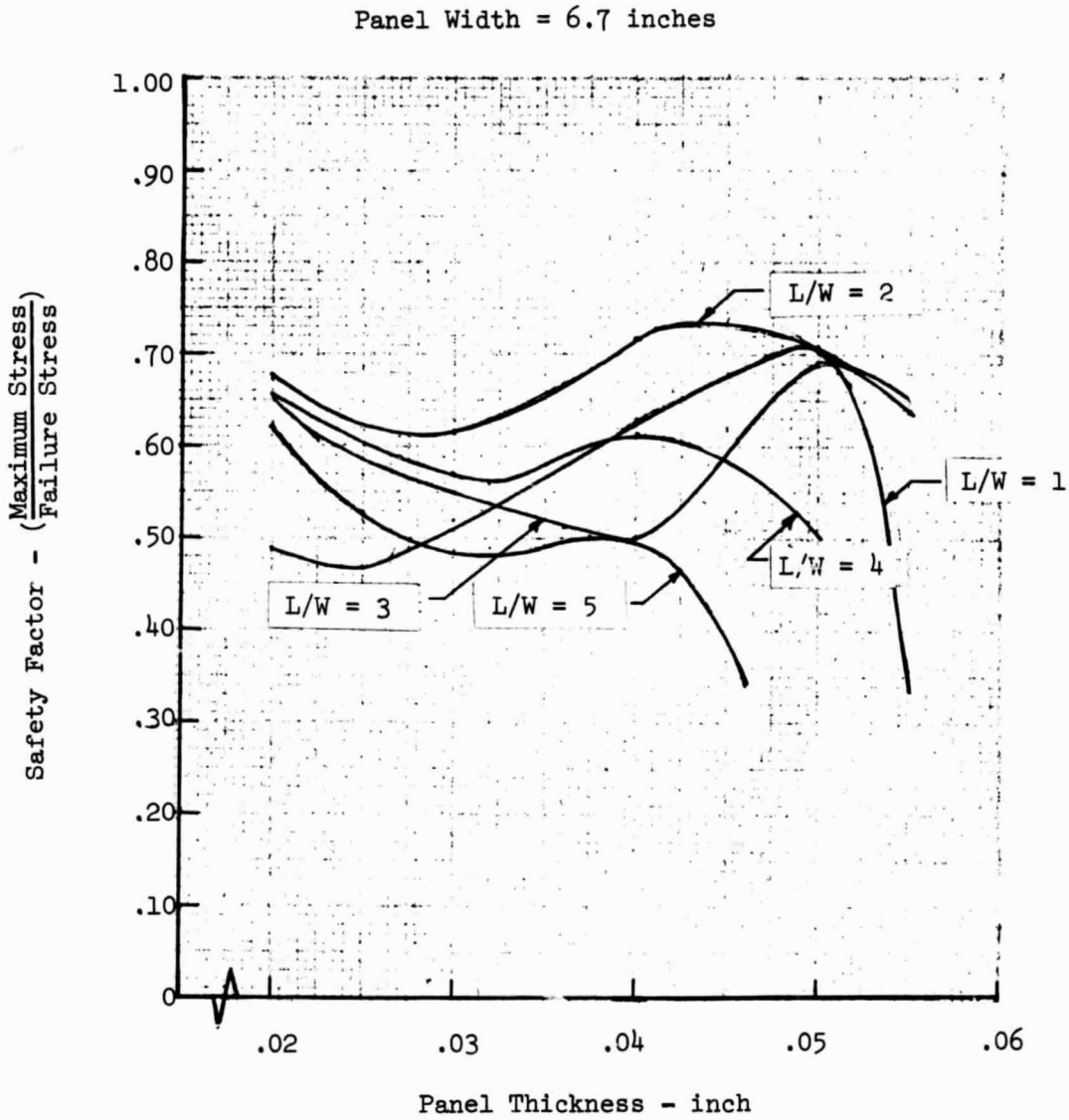


Figure 15 - Stress Safety Factor as a Function of Panel Geometry

REFERENCES

1. Lemley, Clark E., "Design Criteria for the Prediction and Prevention of Panel Flutter," AFFDL-TR-67-140, Vol. II, August 1968.
2. Ventres, Charles S. "Non-Linear Flutter of Clamped Plates", PhD Thesis, Princeton University, October, 1969.
3. Kappus, H.P., Lemley, C.E., and Zimmerman, N.H., "An Experimental Investigation of High Amplitude Panel Flutter," NASA Technical Report to be released February, 1971.
4. Harris, Cyril M., and Crede, Charles E., Shock and Vibration Handbook, Vol. 2, McGraw-Hill Book Company, Inc., 1961, pp. 24-11, 24-12.
5. Dowell, E.H. and Voss, H.M., "Experimental and Theoretical Panel Flutter Studies in the Mach Number Range of 1.0 to 5.0," Technical Documentary Report No. ASD-TDR-63-449, December, 1963.
6. Hess, R.W. "Experimental and Analytical Investigation of the Flutter of Flat Built-up Panels under Streamwise Inplane Load," NASA TR R-330, February, 1970.
7. Hodson, C.H. and Stocker, J.E., "Supersonic Transport Panel Flutter Studies," Technical Documentary Report No. RTD-TDR-63-4036, May, 1964.
8. Voss, H.M. and Ketter, D.J., "Flutter Analyses and Experiments in the Mach Number Range of 5.0 to 10.0," Technical Documentary Report No. FDL-TDR-64-6, March, 1964.
9. Timoshenko, S. and Woinowsky-Krieger, S., Theory of Plates and Shells 2nd Edition, McGraw-Hill Book Company, 1959, pp. 421-425.
10. Young, Dana, "Vibration of Rectangular Plates by the Ritz Method," Journal of Applied Mechanics, December 1950, pp. 448-453.
11. Peterson, R.E., Stress Concentration Design Factors, John Wiley and Sons, 1953.
12. Metallic Materials and Elements for Aerospace Vehicle Structures, Mil-HDBK-5A, 5 January 1970, p 3.3.1 (r).
13. "Saturn V Launch Vehicle Panel Flutter AS-504," Boeing Company Report D5-15358-4A, 5 March 1969.
14. Gaspers, Peter A., Muhlstein, Lado, and Petroff, Daniel N., "Further Experimental Results on the Influence of Turbulent Boundary Layer on Panel Flutter," NASA TN D-5798, May 1970.